cooled to −78 °C. A solution of 50% D_2O–CF_3CO_2D was added, and stirring was continued for 20 min. A 0.2 mM solution of *N*-phenyltriazolinedione in acetonitrile was added dropwise until the pink color persisted. The product **7** was isolated by extractive isolation (CH_2Cl_2–H_2O) and purified by preparative TLC (silica, $CHCl_3$). MS (CI, NH_3): *m/e* 387 ($M + NH_4^+ + 2$, 30%), 386 ($M + NH_4^+ + 1$, 100%), 385 ($M + NH_4^+$, 80%). ^1H NMR (200 MHz, $CDCl_3$): δ 7.5–7.3 (m, not integrated), 6.46 (m, integral = 35), 5.14 (m, integral = 32), 4.40 (br s, integral = 11).

Kinetics. A solution of iodobenzene at 5.0 or 0.50 mM (internal standard) with various concentrations (cf. Table I) of tetrabutylammonium halide in acetonitrile was prepared (solution A). Another solution (solution B) was prepared of 5.0–50 mM substrates **1–4** in CCl_4. Equal volumes of solutions A and B were combined, shaken, and incubated at 25.0 °C in a temperature bath. Aliquots (250 mL) were periodically removed and filtered through 0.4–0.6 g of silica in a Pasteur pipet, eluting with 1.2 mL of CCl_4. The eluant was frozen in dry ice until it could be analyzed by gas chromatography.

Gas chromatographic analysis was carried out with a Varian Model 3700 gas chromatograph equipped with a 30 m × 1.5 μm DB1 column and FID detector. The injector temperature was maintained at 200 °C (higher temperatures resulted in 1,5-proton migration in the cyclopentadienes). The aliquot was warmed to ambient temperature, and either 0.5 or 1.0 μL was injected, depending on the anticipated concentration of the species to be assayed. One of three temperature gradient programs was initiated: (a) 40 °C for 2 min, increase 30 deg/min until 200 °C (halocyclopentadienes); (b) 45 °C for 2 min, increase 30 deg/min until 200 °C (cyclopentyl iodide); (c) 70 °C for 3 min, increase 40 deg/min until 200 °C (cyclopentyl bromide). Every attempt was made to maintain consistency of injection size, temperature program, and peak integration technique within each run, and for the calibration curve for that run.

The ratios of the integrated peaks corresponding to appearing product and internal standard were determined. These data and the relative response factor for the product versus the internal standard were used to calculate the initial rate for each reaction in the standard way. Reactions were followed only until 5% of the starting alkyl halide had disappeared, so no logarithmic plot was required. At high nucleophile concentrations and especially with compound **3** the depletion of the starting cyclopentadienyl halide due to 1,5-proton migration was rapid, and the initial rate was extrapolated from a plot of the observed rate vs time.

Acknowledgment. This work has been supported by a grant from the National Science Foundation and by an NIH postdoctoral fellowship to J.C.

Modular Design of Synthetic Protein Mimics. Crystal Structure of Two Seven-Residue Helical Peptide Segments Linked by ϵ-Aminocaproic Acid

Isabella L. Karle,*,† Judith L. Flippen-Anderson,† M. Sukumar,‡ K. Uma,‡ and P. Balaram*,‡

Contribution from the Laboratory for the Structure of Matter, Naval Research Laboratory, Washington, D.C. 20375-5000, and the Molecular Biophysics Unit, Indian Institute of Science, Bangalore-560 012, India. *Received November 9, 1990*

Abstract: Two seven-residue helical segments, Val-Ala-Leu-Aib-Val-Ala-Leu, were linked synthetically with an ϵ-aminocaproic acid (Acp) linker with the intention of making a stable antiparallel helix–helix motif. The crystal structure of the linked peptide Boc-Val-Ala-Leu-Aib-Val-Ala-Leu-Acp-Val-Ala-Leu-Aib-Val-Ala-Leu-OMe (**1**) shows the two helices displaced laterally from each other by the linker, but the linker has not folded the molecule into a close-packed antiparallel conformation. Two strong intermolecular NH···O=C hydrogen bonds are formed between the top of the lower helix of one molecule and the bottom of the upper helix in a laterally adjacent molecule to give the appearance of an extended single helix. The composite peptide with Boc and OMe end groups, $C_{76}H_{137}N_{15}O_{18}\cdot H_2O$, crystallizes in space group $P2_1$ with a = 8.802 (1) Å, b = 20.409 (4) Å, c = 26.315 (3) Å, and β = 90.72 (1)°; overall agreement R = 7.86% for 5030 observed reflections ($|F_o| > 3\sigma(F)$); resolution = 0.93 Å. Limited evidence for a more compact conformation in solution consistent with an antiparallel helix arrangement is obtained by comparison of the HPLC retention times and CD spectra of peptide **1** with well-characterized continuous helices of similar length and sequence.

The design and construction of synthetic mimics for folding motifs in proteins has attracted considerable recent interest.[1] A modular approach illustrated in Figure 1 is being developed in these laboratories, which envisages stepwise assembly of conformationally rigid helices into super-secondary structures like the α,α motif by means of intervening flexible linker sequences.[2] This strategy relies on the ability of α-aminoisobutyric acid (Aib)[3] to stabilize helical structures in oligopeptides.[4] The systematic investigation of the effects of Aib content, precise positioning of Aib residues, chain length, and sequence have led to the synthesis and characterization in crystals of several helical oligopeptides.[5] These peptides have yielded predominantly α-helical conformations, ranging in length from 2 to 4 helical turns, and can serve, in principle, as the structurally defined modules in further assembly. In this paper we describe the joining of two helical segments by a flexible linker residue, ϵ-aminocaproic acid (Acp). The two end moieties of the linker, NH and $C^{\alpha}H_2C{=}O$, should provide hydrogen bonding groups that serve to continue the helical conformation of the individual modules, while the central $(CH_2)_5$

† Naval Research Laboratory.
‡ Indian Institute of Science.

(1) (a) DeGrado, W. F. *Adv. Protein Chem.* **1988**, *39*, 51–124. (b) DeGrado, W. F.; Wasserman, Z. R.; Lear, J. D. *Science* **1989**, *243*, 622–628. (c) Hill, C. P.; Anderson, D. H.; Wesson, L.; DeGrado, W. F.; Eisenberg, D. *Science* **1990**, *249*, 543–546. (d) Hecht, M. H.; Richardson, J. S.; Richardson, D. C.; Ogden, R. C. *Science* **1990**, *249*, 884–891. (e) Kaumaya, P. T. P.; Berndt, K. D.; Heidorn, D. B.; Trewhella, J.; Kezdy, F. J.; Goldberg, E. *Biochemistry* **1990**, *29*, 13–23. (f) Hahn, K. W.; Klis, W. A.; Stewart, J. M. *Science* **1990**, *248*, 1544–1547. (g) Mutter, M.; Vuilleumier, S. *Angew. Chem., Int. Ed. Engl.* **1989**, *28*, 535–554. (h) Sasaki, T.; Kaiser, E. T. *J. Am. Chem. Soc.* **1989**, *111*, 380–381.

(2) (a) Karle, I. L.; Flippen-Anderson, J. L.; Uma, K.; Balaram, P. *Biochemistry* **1989**, *28*, 6696–6701. (b) Karle, I. L.; Flippen-Anderson, J. L.; Uma, K.; Balaram, P. *Curr. Sci.* **1990**, *59*, 875–885. (c) Karle, I. L.; Flippen-Anderson, J. L.; Uma, K.; Sukumar, M.; Balaram, P. *J. Am. Chem. Soc.* **1990**, *112*, 9350–9356.

(3) (a) Abbreviations used: Aib, α-aminoisobutyric acid; Acp, ϵ-aminocaproic acid; Boc, (*tert*-butyloxy)carbonyl. (b) For definitions of torsional angles, see: IUPAB-IUB Commission on Biochemical Nomenclature. *Biochemistry* **1970**, *9*, 3471–3479. (c) All chiral amino acids are of the L configuration.

0002-7863/91/1513-3952$02.50/0

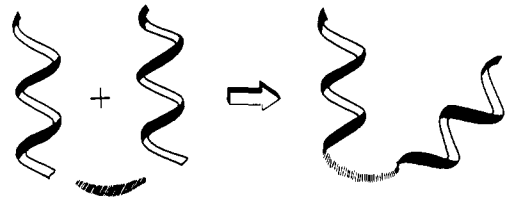

Figure 1. Schematic diagram of the desired conformation about a linker between two helices for an α,α motif.

hydrocarbon chain should provide sufficient flexibility for chain folding. The helical module chosen has the sequence -Val-Ala-Leu-Aib-Val-Ala-Leu- and has been previously characterized in crystals with the terminal Boc and methyl ester protecting groups.[6] The crystal structure of the linked peptide Boc-Val-Ala-Leu-Aib-Val-Ala-Leu-Acp-Val-Ala-Leu-Aib-Val-Ala-Leu-OMe (**1**) reveals two distinct helical segments, which have approximately parallel helical axes.

Experimental Procedures

Peptide **1** was synthesized by coupling Boc-Val-Ala-Leu-Aib-Val-Ala-Leu-OH to Acp-OMe with dicyclohexylcarbodiimide and 1-hydroxybenzotriazole, under standard conditions,[7] followed by base hydrolysis of the resultant peptide ester and coupling of the peptide acid thus obtained to the free base H-Val-Ala-Leu-Aib-Val-Ala-Leu-OMe. The heptapeptide acid and free bases were obtained from the corresponding fully protected peptide Boc-Val-Ala-Leu-Aib-Val-Ala-Leu-OMe[6] by saponification (2 N NaOH/MeOH) or by formic acid deprotection, respectively. Standard coupling, deprotection, and workup procedures were used as described elsewhere for related peptides.[7]

Peptide **1** was purified by reverse-phase HPLC on a C_8 column, using methanol–water gradient elution, and obtained as a white crystalline solid, mp 130–133 °C. The peptide was fully characterized by two-dimensional ^{1}H NMR at 270 MHz with all fifteen NH resonances being clearly recognized in $CDCl_3$ solutions. Thirteen C$^\alpha$H–NH cross peaks were observed in a COSY spectrum, while the two Aib NH resonances are singlets.

Clear, colorless crystals were grown by slow evaporation from methanol–water. X-ray diffraction data were measured at room temperature over a period of 4 days on a dry crystal that was freshly removed from its mother liquor. The crystals, both dry and wet, deteriorated in quality after a period of several weeks. During the data collection, three reflections, monitored after every 97 measurements, remained constant within 3%. An automated four-circle diffractometer equipped with a graphite monochromator was used with a $\theta/2\theta$ scan mode, a $2.0° + 2\theta(\alpha_1 - \alpha_2)$ scan, variable scan speeds depending upon the intensity of the reflection, and $2\theta_{max} = 110°$ (0.94-Å resolution). Cell parameters and diffraction data are listed in Table I.

The structure was solved by a vector search procedure in the Patsee computer program[8] contained in the SHELX84 package of programs (MicroVAX version of the SHELXTL system of programs, Siemens Instruments, Madison, WI). The model used for the vector search consisted of 24 backbone atoms from the known structure of Boc-Val-Ala-Leu-Aib-Val-Ala-Leu-OMe.[6] After rotation and translation to the correct position in the cell, the remainder of the atoms were found with the partial structure procedure.[9] Full-matrix, anisotropic, least-squares refinement was performed on the C, N, and O atoms in the peptide, after which hydrogen atoms were placed in the idealized positions, with C–H = 0.96 Å, and allowed to ride with the C or N atom to which each was bonded for the final cycles of refinement. The thermal factor for the hydrogen atoms was fixed at $U_{iso} = 0.125$. The side chains in Leu(7) and Val(8), as well as the terminal OMe group, are disordered among two positions each (see the occupancy factors in Table II). To facilitate refinement in the disordered regions for Leu(7) and OMe where there is overlap in the electron densities from the disordered positions, the C$^\gamma$–C$^\delta$ and O–Me bond lengths were restrained to 1.52 and 1.45 Å, respectively. Occupancy factors were refined. In Val(8) where one of the C$^\gamma$ atoms occupies two different positions, all parameters, including the occupancy factor, were allowed to vary. The final R factor for 5030 data was 7.86%.

Fractional coordinates for the C, N, and O atoms are available in the supplementary material. Bond lengths and bond angles (esd's ~0.015 Å for bonds and 1.0° for angles) do not show significant or systematic differences from expected values.

Table I. Diffraction and Crystal Parameters for Boc-Val-Ala-Leu-Aib-Val-Ala-Leu-Acp-Val-Ala-Leu-Aib-Val-Ala-Leu-OMe

empirical formula	$C_{76}H_{137}N_{15}O_{18}\cdot H_2O$
crystallizing solvent	CH_3OH/H_2O
color/habit	colorless prism
crystal size, mm	0.2 × 0.4 × 0.5
space group	$P2_1$
cell parameters	
a, Å	8.802 (1)
b, Å	20.409 (4)
c, Å	26.315 (3)
β, deg	90.72 (1)
vol, Å^3	4727.0
Z	2
formula wt	1549.05 + 18.0
density (calcd), g/cm^3	1.101
$F(000)$	1704
temperature	ambient
mounted in capillary	no
radiation	Cu Kα (λ = 1.54184 Å)
2θ range, deg	1–112
resolution, Å	0.93
scan type	θ–2θ
scan speed, deg/min	7.10
scan range	2.0° + Kα separation
index range	
h	−9 to 9
k	−21 to 4
l	0 to 28
independent reflcns	6491
obsd reflcns [$\lvert F_o\rvert > 3\sigma(E)$]	5030
final R indices (obsd data)	R = 7.86%; wR = 8.21%
no. of parameters refined	1038
data to parameter ratio	4.8–1.0
largest difference peak e Å^{-3}	0.23
largest difference hole e Å^{-3}	−0.25

Table II. Hydrogen Bonds[g]

type	donor	acceptor	N···O, Å	H···O,[a] Å	C=O···N angle, deg
head-to-tail	N(1)	O(13)[b]	2.887	1.93	
	N(2)	W(1)[c]	2.947	2.02	
4→1	N(3)	O(0)	3.035	2.20	130
	N(4)	O(1)	3.078	2.46	118
	N(5)				
5→1	N(6)	O(2)	2.931	2.04	154
	N(7)	O(3)	2.994	2.07	159
	N(Acp)	O(4)	2.912	2.06	148
intermolecular	N(8)	O(6)[d]	2.919	1.97	138
	N(9)	O(7)[d]	2.890	2.05	153
4→1	N(10)	O(Acp)	3.176	2.69	114
5→1	N(11)	O(Acp)	2.900	1.97	166
	N(12)	O(8)	3.292	2.38	152
	N(13)	O(9)	3.313	2.49	145
	N(14)	O(10)	2.902	2.18	164
water–peptide	W(1)	O(12)[e]	2.801[f]		
	W(1)	O(15)[e]	3.038[f]		

[a] Hydrogen atoms have been placed in idealized positions with N–H = 0.96 Å. [b] Symmetry equivalent $1 + x, y, -1 + z$ to coordinates listed in supplementary material. [c] Symmetry equivalents $2 - x, {}^1/_2 + y, -z$ to coordinates listed in supplementary material. [d] Symmetry equivalents $-1 + x, y, z$ to coordinates listed in supplementary material. [e] Symmetry equivalents $1 - x, -{}^1/_2 + y, 1 - z$ to coordinates listed in supplementary material. [f] O···O distance. [g] Atoms O(5), O(11), O(14), and N(5) do not participate in any hydrogen bonding. Atom N(10) may make a poor 4→1 hydrogen bond with O(Acp), although the H···O distance is long and the C=O···N angle is small.

(4) (a) Nagaraj, R.; Balaram, P. *Acc. Chem. Res.* **1981**, *14*, 356–362. (b) Prasad, B. V. V.; Balaram, P. *CRC Crit. Rev. Biochem.* **1984**, *16*, 307–348. (c) Uma, K.; Balaram, P. *Ind. J. Chem.* **1989**, *28B*, 705–710. (d) Marshall, G. R.; Hodgkin, E. E.; Lang, D. A.; Smith, D. G.; Zabrocki, J.; Leplawy, M. T. *Proc. Natl. Acad. Sci. U.S.A.* **1990**, *87*, 487–491. (e) Toniolo, C.; Benedetti, E. *ISI Atlas of Science: Biochemistry* **1988**, *1*, 225–230.

(5) Karle, I. L.; Balaram, P. *Biochemistry* **1990**, *29*, 6748–6756.

(6) Karle, I. L.; Flippen-Anderson, J. L.; Uma, K.; Balaram, P. *Proteins: Struct., Funct. Genet.* **1990**, *7*, 62–73.

(7) (a) Balaram, H.; Sukumar, M.; Balaram, P. *Biopolymers* **1986**, *25*, 2209–2223. (b) Sukumar, M. Ph.D. Thesis, Indian Institute of Science, Bangalore, 1987. (c) Uma, K. Ph.D. Thesis, Indian Institute of Science, Bangalore, 1990.

(8) Egert, E.; Sheldrick, G. M. *Acta Cryst.* **1985**, *A41*, 262–268.

(9) Karle, J. *Acta Crystallogr.* **1968**, *B24*, 182–186.

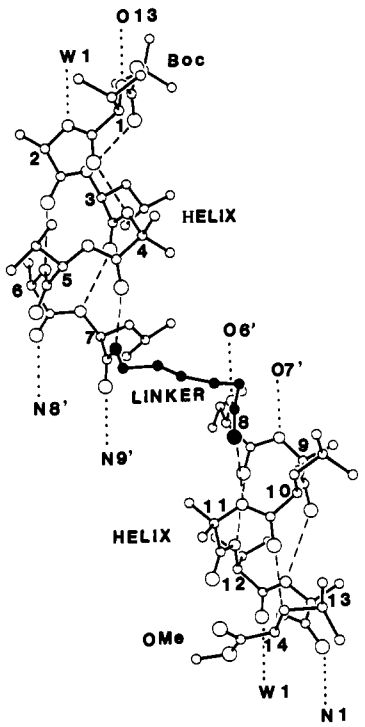

Figure 2. The structure of Boc-Val-Ala-Leu-Aib-Val-Ala-Leu-Acp-Val-Ala-Leu-Aib-Val-Ala-Leu-OMe (**1**) as determined by crystal structure analysis. Intramolecular NH···O=C bonds in the helices are indicated by dashes. Intermolecular hydrogen bonds are indicated by dots. The atoms in the ε-aminocaproic (Acp) linker are shown darkened. The water molecule in the heat-to-tail region is designated by W1. The C^{α} atoms are numbered 1–14. For the disorder in the side chains in residues 7 and 8, and in the OMe at the C terminus, only one orientation is shown.

Results

The Peptide Molecule. The seven-residue peptide segments at the N and C ends of the molecule fold into a mixed $3_{10}/\alpha$-helix, respectively, with conformations close to that found in the isolated seven-residue peptide with the same sequence, Boc-Val-Ala-Leu-Aib-Val-Ala-Leu-OMe.[6] The Acp linker portion offsets laterally one helical segment from the other (Figure 2). The magnitude of the offset is such that the upper helix segment of one molecule is placed over the lower helix segment of a neighboring molecule (Figure 3). Two intermolecular NH···O=C hydrogen bonds at the centers of the molecules, N(8)···O(6) and N(9)···O(7) (see Table II and Figures 2 and 3), connect the two helices from separate molecules into an extended helix. Furthermore, head-to-tail hydrogen bonding in the form of a direct N(1)···O(13) bond and water mediated hydrogen bonds N(2)···W(1) and W(1)···O(12) connect the helical segments into continuous helical columns parallel to the z axis.

The upper helix in the molecule (Figure 2) has two 4 → 1 (3_{10} type) hydrogen bonds, N(3)···O(0) and N(4)···O(1). In the transition region between the 3_{10}- and α-helix, N(5) does not participate in any hydrogen bonding. The helix continues as an α-type with three 5→1 hydrogen bonds, N(6)···O(2), N(7)···O(3), and N(Acp)···O(4) where N(Acp) is part of the linker molecule. At the other end of the linker, C=O(Acp) participates in a 5→1 hydrogen bond with N(11) in the lower helix. Three additional 5→1 hydrogen bonds, N(12)···O(8), N(13)···O(9), and N(14)···O(10), complete the lower α-helix. At the top of the lower helix, N(8) and N(9) form hydrogen bonds with O(6) and O(7) of the bottom of the upper helix from a neighboring molecule as described in the previous paragraph and shown in Figure 2. A weak and distorted hydrogen bond may also exist between N(10) and O(Acp), but the H···O distance at 2.69 Å is much longer than any other H···O distance shown in Table II.

Torsion angles ϕ, ψ, and ω for the helical backbones fall within the range that has been observed for many other helical peptides containing one or several Aib residues.[5] Disorder in side chains of apolar helical peptides, as found for Leu(7) and Val(8) on either side of the linker region and for the OMe end group, is not unusual. The existence of such disorder implies loose packing in the crystal and weak van der Waals' attractions between molecules.

Crystal Packing. The molecule repeats along the x direction, the direction of the offset helices, as shown in Figure 3. Furthermore, there is head-to-tail hydrogen bonding, as described above, so that an extended sheet, one molecule thick, is formed. The N termini of all the peptide molecules in any particular sheet are directed in the same direction. The sheets of molecules are perpendicular to the y axis of the crystal. The 2-fold screw operation along the y axis results in turning adjacent sheets antiparallel to each other. There is no hydrogen bonding between sheets. Figure 4 shows the two molecules in a unit cell. The view down the z axis, and also down the helix axes, shows one helix near the top of the diagram and the other helix near the bottom with the Acp linker near the middle. The molecule at the left is contained in one sheet that is parallel to the XZ face, and the molecule on the right is in a different sheet where the molecules are oriented in an antiparallel fashion to those of the left. All the contacts between sheets are entirely hydrophobic, between CH_3···CH_3 or CH_2···CH_3 moieties, with closest C···C approaches ranging between 3.8 and 4.1 Å. Between the sheets, the nearest approaches occur between Val···Val side chains and Leu···Leu side chains. Within a sheet, the repeating peptide molecules have close approaches between Aib···Ala side chains.

The Linker. A diagram of the ε-aminocaproic acid residue, used as a linker between the two residue helices, is shown in Figure 5 in the same orientation as is shown in Figure 4, right-hand

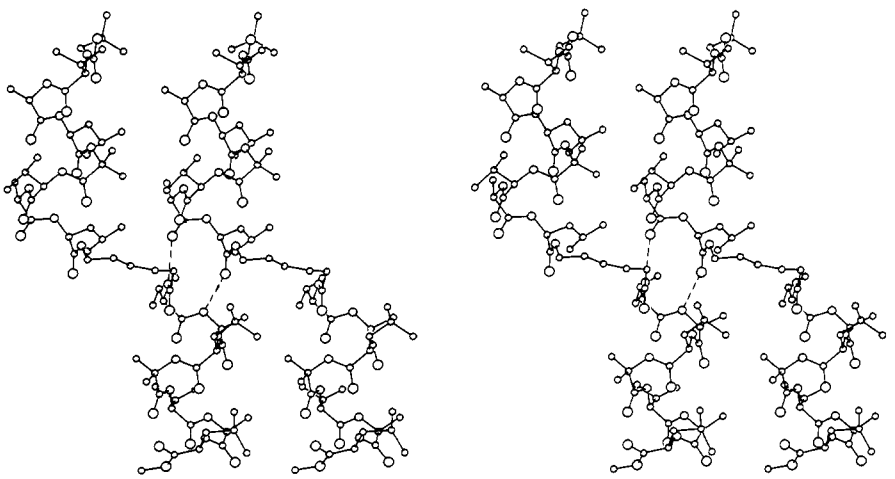

Figure 3. Stereodiagram of two repeating peptides in the same orientation as in Figure 2. The axial directions of the cell are x (→) and z (↓). The only hydrogen bonds shown are those linking the bottom helix of one peptide molecule with the top helix of the neighboring peptide molecule.

Table III. Torsion Angles (deg)[a,b]

residue	ϕ	ψ	ω	χ^1	χ^2	χ^3	χ^4	χ^5
Val(1)	−66[c]	−25	176	−62, 65				
Ala(2)	−55	−35	180					
Leu(3)	−60	−44	−177	178	65, −169			
Aib(4)	−56	−44	−179					
Val(5)	−77	−35	179	−49, −172				
Ala(6)	−65	−35	−178					
				−148	32, 169			
Leu(7)[d]	−88	−48	180[e]	−83	−59, 180			
Acp(A)[f]		+123	−177	−63	−162	−164	−62	117
				68				
Val(8)[d]	−62	−40	−178	−176, −59				
Ala(9)	−68	−37	176					
Leu(10)	−65	−46	−176	−67	177, −62			
Aib(11)	−54	−48	−172					
Val(12)	−78	−22	179	−62, 67				
Ala(13)	−88	−18	−179					
		+53	−170					
Leu(14)[g]	−127	−116	+159	−69	162, −67			

[a] The torsion angles for rotation about bonds of the peptide backbone (ϕ,ψ,ω) and about bonds of the amino acid side chains (χ^n) are described in ref 3b. [b] Esd's ~1.0°. [c] C′(0), N(1), C^α(1), C′(1). [d] Disordered side chains. [e] C^α(7), C′(7), N^ζ(A)C^ϵ(A). [f] Torsions in *main chain* in the linker Acp about C^α–C^β, C^β–C^γ, C^γ–C^δ, C^δ–C^ϵ, and C^ϵ–N^ζ are designated as χ^1 to χ^5, respectively. [g] Disordered OMe: $\psi \equiv$ N(14)C^α(14)C′(14)O(OMe); $\omega \equiv$ C^α(14)C′(14)O(OMe)C(OMe).

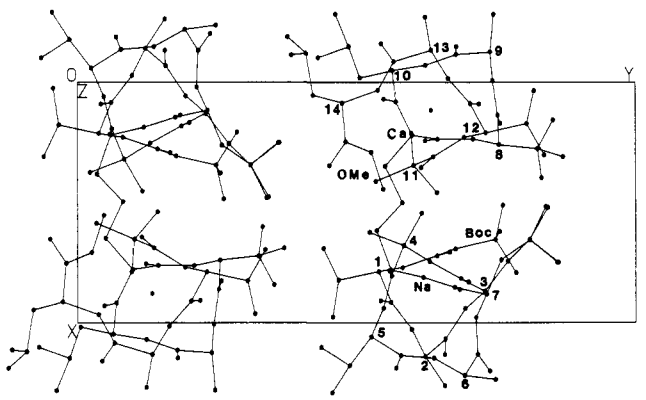

Figure 4. A view down the *z* axis, looking into the helices, of the two molecules in the cell related by a 2-fold screw operation along the *y* direction. Atoms labeled Na and Ca are the N and C^α atoms of the Acp linker. Labels 1–14 refer to the C^α atoms of the two 7-residue helices of the peptide.

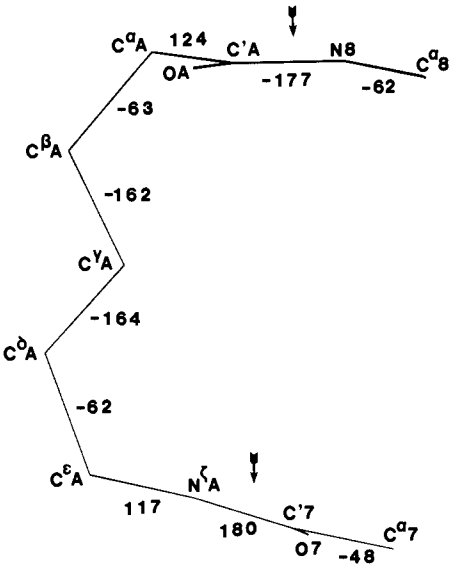

Figure 5. The Acp linker, bounded by the arrows, between residues 7 and 8. The orientation is the same as in the right-hand molecule in Figure 4. The numbers denote the torsion angles about the bonds.

molecule. The torsional angles for the linker, indicated in Figure 5 and listed in Table III, are completely symmetric about C^γ(A). The *gttg* conformation for the C^α(A)–C^ϵ(A) portion of the linker is not unusual for a $(CH_2)_5$ segment. It is stabilized further by the serendipitous formation of the intermolecular hydrogen bonds N(8)···O(6) and N(9)···O(7) which effectively link the 7-residue helices from different molecules into a continuous helix that traverses the crystal. Interestingly, the two gauche conformations observed about the C^α–C^β and C^δ–C^ϵ bonds of the linker are also a feature of all ten computed low-energy conformations of the cyclized β-bend model, *cyclo*(Ala-Gly-Acp).[10]

Rotations about C^α(A)–C^β(A) and/or C^δ(A)–C^ϵ(A) can be performed on models, resulting in *all-trans* linker conformation, that bring both helical portions in close proximity to each other as shown schematically in Figure 1.

A comparison of the HPLC retention times of **1** with those of several related peptides, under identical conditions (Table IV), reveals that **1** elutes appreciably faster from the octadecylsilica column, in contrast to long, continuous helices of similar length and sequence. This suggests that in solution, **1** may adopt a more compact conformation, which minimizes the surface area in contact with the hydrophobic alkyl chain of the stationary phase. Figure 6 shows the CD spectra of **1**, its heptapeptide precursor, the related 14-residue sequence lacking the central Acp linker, and a 15-residue peptide containing an additional Aib residue. It is clearly seen that the 14- and 15-residue peptides yield CD spectra characteristic of largely helical conformations.[11] The

Table IV. HPLC Retention Times and Crystal Conformation of Helical Peptides

peptide[a]	retention time,[b] min	solid-state conformation[c]
Boc-VALUVAL-Acp-VALUVAL-OMe	19.2	A[d]
Boc-(VALUVAL)$_2$-OMe	27.4	*e*
Boc-(VALUVAL)$_2$U-OMe	31.2	A (ref 2c)
Boc-(VALUVALU)$_2$-OMe	33.0	A (ref 2c)
Boc-VALUVAL-OMe	13.5	A, A(W)[f] (ref 6)
Boc-(VALU)$_2$-OMe	15.1	A, A/T[f] (ref 6)

[a] Single-letter code: V, Val; A, Ala; L, Leu; U, Aib. [b] Gradient of 80–95% MeOH in 15 min on a Shimpack CLC ODS (6 × 150 mm, 5 μm) column. Flow, 0.8 mL min^{-1}; detection, 226 nm. [c] A, totally or predominantly α-helix; T, 3_{10}-helix; A/T, mixed $\alpha/3_{10}$-helix; (W), water inserted into backbone. Crystals have been obtained from methanol/water systems. [d] Present paper. [e] Structure not yet available. [f] Two molecules in the asymmetric unit.

(10) Némethy, G.; McQuie, J. R.; Pottle, M. S.; Scheraga, H. A. *Macromolecules* **1981**, *14*, 975–985.

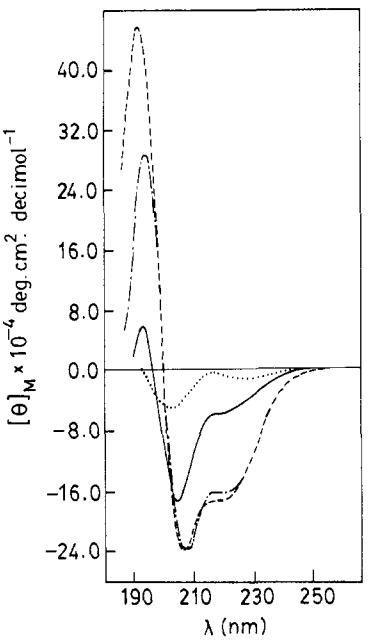

Figure 6. Circular dichroism spectra of **1** and related compounds, in methanol: (—) Boc-Val-Ala-Leu-Aib-Val-Ala-Leu-Acp-Val-Ala-Leu-Aib-Val-Ala-Leu-OMe; (-·-) Boc-(Val-Ala-Leu-Aib-Val-Ala-Leu)$_2$-OMe; (- - -) Boc-(Val-Ala-Leu-Aib-Val-Ala-Leu)$_2$-Aib-OMe; (···) Boc-Val-Ala-Leu-Aib-Val-Ala-Leu-Ome. Peptide concentration, 1 mg/mL. CD spectra were recorded on a JASCO J500A spectropolarimeter with 0.1 mm path length cells. Signal averaging was performed and spectra are corrected for the solvent baseline obtained under the same conditions.

7-residue fragment displays very low ellipticity values in the far-UV region (190–230 nm), suggestive of a largely unordered structure. Although a helical structure has been observed for this peptide in crystals, NMR evidence suggests a greater conformational variability in solution.[6,7c] Peptide **1** has significantly higher ellipticity values at 220, 205, and 194 nm, as compared to the heptapeptide, but much lower values when compared to the 14- and 15-residue peptides. This observation is consistent with a greater helical content of the two heptapeptide modules in **1**, relative to the isolated heptapeptide. This may, indeed, be a consequence of a compact folded structure, which stabilizes the helical backbones of the two segments in solution.

Discussion

This attempt at constructing a system of two linked α-helices has been partially successful. While the continuous helical rod conformation has indeed been broken by the introduction of the central flexible linker, a close-packed, antiparallel helix orientation has not been achieved in crystals. Rather, the solid-state conformation still reveals an elongated molecule. This structure is probably stabilized by the "head-to-tail" hydrogen bonds formed between the termini of the N-terminal helix of one molecule and the C-terminal helix of a neighbor. Limited evidence in favor of a more compact conformation is obtained in solution, suggesting an antiparallel helix arrangement with contacts between the two modules. It is indeed reasonable to expect that compact structures which minimize the solvated surface area are favored in solution. An interesting recent example of dimerization of molecules with large *apolar* surfaces in organic solvents, driven by "*solvophobic*" interactions is provided by studies on cavitands.[12] The repetitive nature of the sequence of peptide **1** does not lend itself to more detailed characterization in solution, by observation of interhelical nuclear Overhauser effects. Efforts are underway to construct molecules with readily assignable side chain proton resonances.

A feature of peptide **1** is the completely apolar nature of the sequence. This facilitates dissolution in organic solvents, where hydrophobic interactions no longer determine the orientation between secondary structure elements. Control of spatial disposition of helices must eventually require either control of linker conformation or the building of specific favorable interactions between the helical modules. Studies in this direction are in progress.

Implications from crystal structure analyses for self-assembly of helices are still indefinite. For helices containing only apolar residues (10–16 residues) all parallel assemblies occur as well as antiparallel assemblies, even for the same peptide crystallized in different crystal forms.[13] For amphiphilic helices, such as the 16-residue Leu-zervamicin,[14] hydrogen bonding between side chains in adjacent peptides plays a major role in association. In a 12-residue fragment of a helix designed to form helical tetramers, which contains both polar and apolar residues, a rather complex association of antiparallel dimers into tetramers and hexamers occurs.[1c] The folding of the present apolar structure into an antiparallel helical entity would not be inconsistent with the present knowledge of self-assembly.

Acknowledgment. This research was supported in part by the National Institutes of Health Grant GM30902, by the Office of Naval Research, and by a grant from the Department of Science and Technology, India.

Supplementary Material Available: Tables of atomic coordinates, bond lengths, bond angles, anisotropic displacement coefficients, and H atom coordinates (11 pages); listing of observed and calculated structure factors (24 pages). Ordering information is given on any current masthead page.

(11) (a) Woody, R. W. In *The Peptides: Conformation in Biology and Drug Design*; Hruby, V. J., Ed.; Academic Press: Orlando, FL, 1985; Vol. 5, pp 15–114. (b) Sudha, T. S.; Vijayakumar, E. K. S.; Balaram, P. *Int. J. Peptide Protein Res.* **1983**, *22*, 464–468.

(12) (a) Bryant, J. A.; Knobler, C. B.; Cram, D. J. *J. Am. Chem. Soc.* **1990**, *112*, 1254–1255. (b) Bryant, J. A.; Ericson, J. L.; Cram, D. J. *Ibid* **1990**, *112*, 1255–1256.

(13) (a) Karle, I. L.; Flippen-Anderson, J. L.; Sukumar, M.; Balaram, P. *Int. J. Peptide Protein Res.* **1990**, *35*, 518–526. (b) Karle, I. L.; Flippen-Anderson, J. L.; Uma, K.; Balaram, P. *Biopolymers* **1990**, *29*, 1835–1845.

(14) Karle, I. L.; Flippen-Anderson, J. L.; Agarwalla, S.; Balaram, P. *Proc. Natl. Acad. Sci. U.S.A.* To be published.